Carleton University
Dept. of Mechanical and Aerospace Engineering

MAAE 4907 C
Prof. M. El Sayed
Prof. P. Liu
Prof R. Liu

Written By:
Eithin Pero
101203184

Reviewed By:
Ibrahim Al-Buhaisi
101191701

Report #: BWB24-TR1-5.7.2

SYSTEMS ENGINEER - 2

FALL 2024 TECHNICAL REPORT

ABSTRACT

This document describes the work accomplished in the fall semester by the Systems Engineer with respect to the mapping module, landing gear, and modelling for the Peregrine 1, a blended-wing body unmanned aerial vehicle (BWB UAV). The current year design emphasizes the use of additive manufacturing, solar powered flight, and a mapping mission. Aerial mapping theory and the current state of the mapping module design decisions are outlined in Section 2.0. The landing gear system design methodology and the current initiatives are described in Section 3.0. A brief overview of the challenges faced, and solutions employed with regards to the Peregrine 1 model is provided in Section 4.0 and is further detailed in the technical document outlining the Peregrine 1 modelling guide, to be published in the winter semester.

TABLE OF CONTENTS

LIST OF TABLES

LIST OF FIGURES

NOMENCLATURE

BWB	Blended-Wing Body
CFD	Computational Fluid Dynamics
DIY	Do It Yourself
FEA	Finite Element Analysis
FOV	Field of View
GCP	Ground Control Point
GPS	Global Positioning System
GSD	Ground Sample Distance
IMU	Inertial Measurement Unit
LiDAR	Light Detection and Ranging
LG	Landing Gear
MB	Megabyte
MP	Megapixel
MSDO	Multiscale Design Optimization
NIR	Near Infrared
OML	Outer Mold Line
P1	Peregrine 1
PETG	Polyethylene Terephthalate Glycol
RGB	Red, Green, Blue
UAV	Unmanned Aerial Vehicle
VTOL	Vertical Takeoff and Landing

1.0 INTRODUCTION

The project objective of the 2024-25 BWB UAV capstone is to design, test, build and fly a solar powered, unmanned aerial vehicle. The blended-wing body configuration of the Peregrine 1 has many benefits for an unmanned, long endurance mission. A blended-wing body aircraft has a seamless transition between the wing and fuselage surfaces, similarly to a flying wing configuration. Contrary to a flying wing, a blended-wing body design retains some semblance to a traditional aircraft by keeping most of the interior volume within the fuselage portion of the body. This design improves the aerodynamic characteristics of the aircraft, allowing the fuselage to generate more lift than the fuselage of the conventional aircraft, improving fuel efficiency [1]. Additionally, with the objective of integrating solar panels onto the body of the wings, the increased area of the upper surface of the body allows the useful placement of more solar panels.

The major design challenges placed upon this years design are the requirements of additive manufacturing, increased flight duration via solar panels, and an optimization of the structure using MSDO principles. The blended-wing body UAV employs a conventional takeoff and landing with a single pusher configuration. Systems Engineers on the team are tasked with the following objectives:

1. Analyzes and designs the power-plant to airframe integration.
2. Analyzes and designs the landing gears to airframe integrations and potentially the deployment and retraction system of the landing gears.
3. Analyzes and designs the control surfaces and their integration into the airframe.
4. Analyzes and designs the mapping module and its integration into the platform.
5. Analyzes and designs the solar panel system and its integration onto the platform body.

An initial allocation of tasks was determined between the two Systems Engineers based on experience and interest. The authors responsibilities included the landing gear tasks, the mapping module, and equal weight between the other Systems Engineer regarding the control surface integration. Due to a high-risk event regarding the CatiaV5 model development of the Peregrine 1, the author was also tasked with assisting in the rectification of the issue.

2.0 MAPPING MODULE

As part of the mission objective for the Peregrine 1, a mapping module was to be designed and implemented to be used in mapping applications.

2.1 Mapping Theory

An initial investigation on the literature review regarding aerial mapping applications was performed. This research lead to a rescope of the authors role regarding the mapping system, noting that the process of designing and testing a mapping system could be an entire capstone in itself. The fundamentals are discussed along with introductions to related considerations that the reader may choose to pursue.

2.1.1 Common Aerial Surveying Uses

Aerial surveying or aerial mapping is used for a very wide range of purposes. Some of the common uses are environmental monitoring, land usage, project development, and agriculture.

2.1.2 Sensors

Many types of sensors exist for data acquisition in the field of aerial imagery and mapping. Any combination of sensors, including but not limited to, LiDAR, RGB optical, Thermal, hyperspectral, multispectral, radar can be used acquire the intended data for a mission.

LiDAR (light detection and ranging) is a type of remote sensing method that uses lasers to measure distances from the observer to the object. The two main configurations for these systems are active and passive, the former employing a source of laser beams to then be recorded as they scatter on the measured surface and the latter sensing ambient waves in the environment. The recorded detections contain information regarding the time it took to return and the direction it was released at. A collection of these measurements can be used to create a 3D point cloud of a scene.

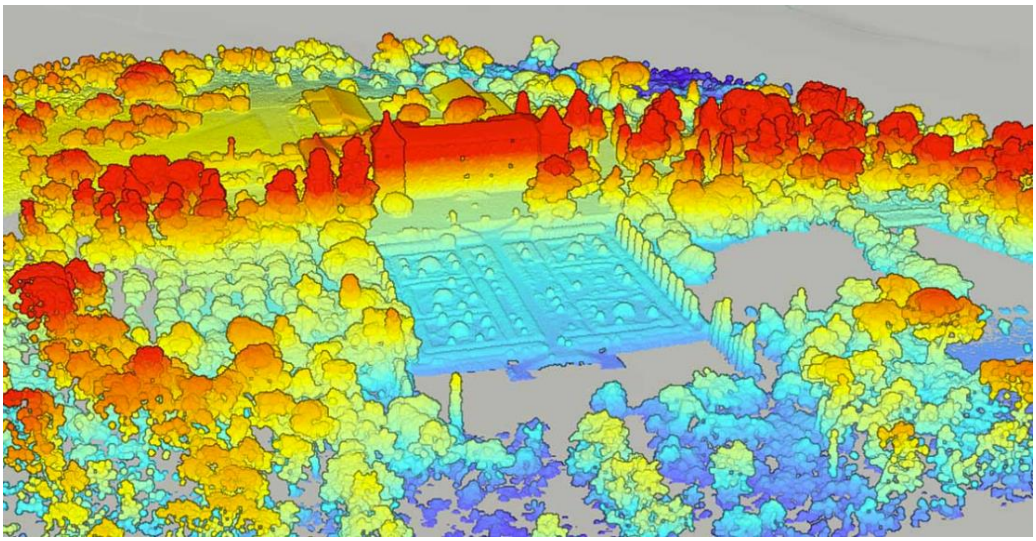

Figure 1: Visualization of 3D point cloud information [2]

The field of optical sensors contains many different types of sensors, each capturing their own bands of light. Disregarding positioning relative to other pixels, an RGB sensor collects only 3 pieces of information for every pixel it captures, a red, green, and blue value. Multispectral and hyperspectral sensors seek to fill in voids of information between these bands of light. In Figure 2 below, it can be seen that the ranges of wavelengths that the RGB sensor is able to detect have much larger voids between them compared to the 8-band sensor. For example, for the range between approximately 675nm and 750nm, the RGB sensor has a poor response compared to the 8-Band NIR sensor, which has a sensor that captures this range with a high response. In addition to adding bands of light in the visible light range, bands can be added from the near infrared, infrared, or ultraviolet regions.

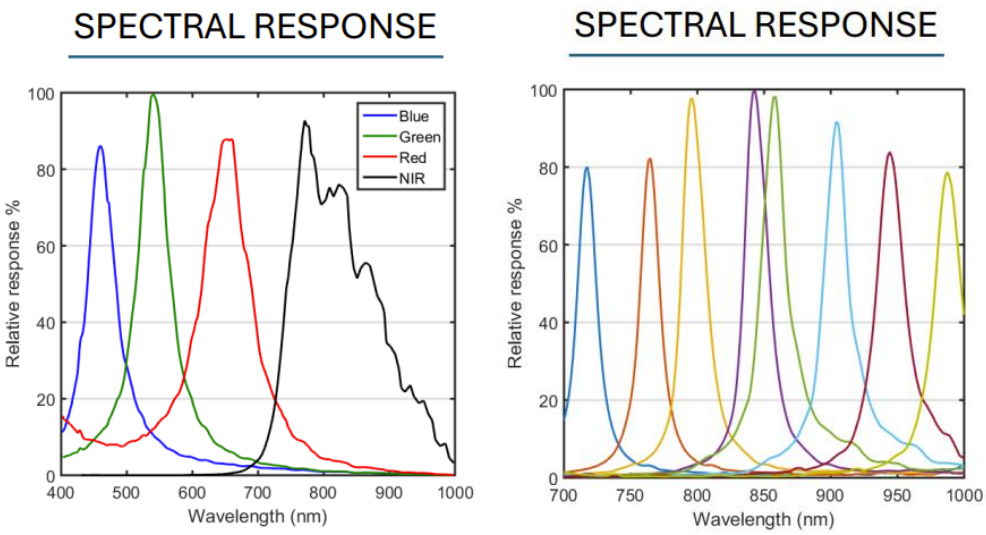

Figure 2: Spectral response of RGB-NIR (left) and 8-band NIR (right) sensors [3]

For agriculteral applications, near-infrared (NIR) bands are commonly used to obtain information about plant health and various plant processes. The most suitable bands for analysis is commonly selected on a case-by-case basis depending on the specific wavelengths the desired information is contained in [4].

2.1.3 Photogrammetry

Photogrammetry is the use of photography in surveying and mapping to measure distances between objects. In a modern context, this word has been used to broadly describe a method of approximating three-dimensional data from a set of two-dimensional images [5]. Essentially, many photos taken from many different angles can be reverse engineered to map to a three-dimensional approximation.

For short distance photogrammetry, stereo cameras can be used to identify distance from an observer, similarily to how our eyes allow depth perception. For aerial mapping, stereo lenses are not very effective due to the comparative difference between the maximum lens spread and the distance to the ground.

From this complication, many softwares and mathematical methods have been developed to reconstruct a three-dimensional scene from images at various positions. Overlap parameters between images can be specified to ensure there will be enough information to accurately map the depth of the terrain and objects. For this reconstruction it is imperative that either accurate GPS and IMU data is recorded for at the time of each image or that ground control points (GCPs) are used to calibrate relative distances, or a combination of the two [6].

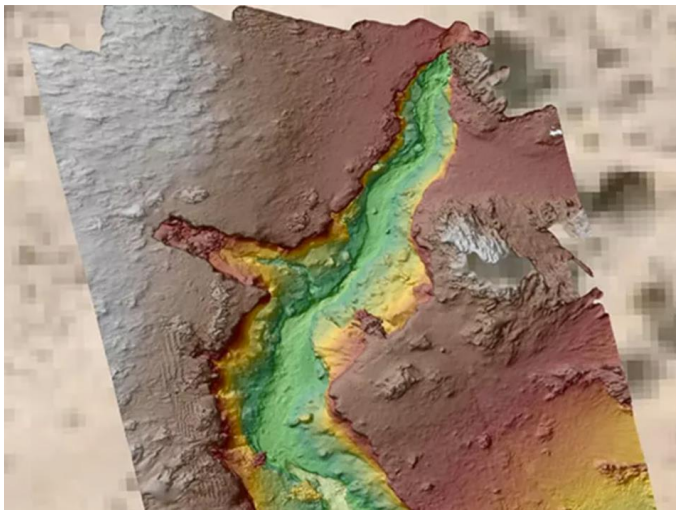

Figure 3: 3D reconstruction of surface feature using photogrammetry [7]

2.1.4 Flight Path

Typically, the desired mapping mission is used to determine the sensor to be used and with this information a suitable platform is chosen [6]. From the sensor properties like the field of view (FOV) and the image resolution, the required ground sample distance (GSD) and footprint can be determined. The GSD is the distance between the centers of two adjacent pixels, measured with respect to the ground [8]. For example, a sensor at 100 ft may have a GSD 10 centimeters, which implies one pixel in an image produced covers a 10x10 area on the ground. Lowering the cruise altitude would allow a smaller ground sample distance, meaning a smaller area covered by a single pixel. The GSD is a function of the camera properties and the cruise altitiude, given in Equation 1 below [8].

$$GSD = \frac{sensor\ width\ [mm] * flight\ height[m]}{focal\ length\ [mm] * image\ width\ [pixels]} \quad (1)$$

The footprint of the camera refers to the total area covered by a single image. Once a required GSD is determined based on the application, a suitable sensor and lens combination is found, and the footprint of each image is determined from the cruising altitude of the platform, the camera perspective centers of the proposed images can be found by fixing the longitudinal and transversal overlap, which is recommended at about 60%-80% of the footprint for photogrammetry uses [6]. Simply put, each image taken along a path must have an overlap with the previous image taken in order for photogrammetry to be performed. If the area of interest is wider than the width of a single footprint, there will be a 180° turn at the edge of the area of interest in the flight path and the footprint overlap in the transverse direction to the flight path must also be considered.

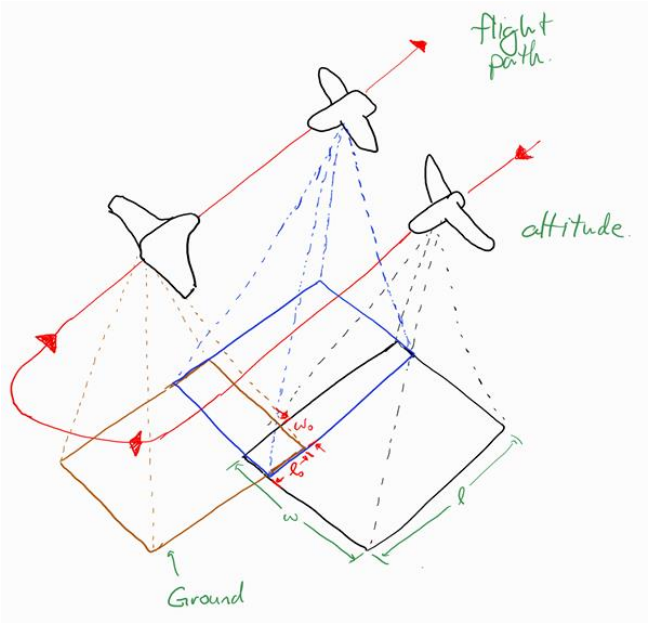

Figure 4: Flight path and footprints

2.1.5 Camera Calibration

Briefly identified was the need for camera calibration. Due to the geometry of optical sensors and lenses, there is a portion at the edge of the lens which is not of true proportions to the actual data. The extreme of this case is seen in a fish-eye lens, where the entire picture is distorted by the curvature of the lens. All lenses have a degree of distortion to them. In the context of aerial imagery and mapping, these effects are amplified due to the distance between the platform and the ground. Additionally, to retrieve accurate distances between objects from images taken with a camera, each distortion must be identified and accounted for accordingly [6].

Many integrated mapping systems are calibrated to their respective lens. If the reader chooses to proceed with a custom mapping system in the future, be aware of the methods and mathematical models used to calibrate vision systems [9].

2.1.6 Data Storage

Once your sensor is chosen, flight path determined, calibration complete, there needs to be some consideration to the method of data storage. The two main categories of options are onboard or live streaming. Onboard storage is the most simple of the two, with its main considerations being the read and write speed of the storage device selected compared to the file size of the images produced. For example, if a picture is needed every 3.5 seconds to comply with the specified overlap parameter, and each picture is approximately 50 MB, the data transfer method and storage device must have a read and write speed of a minimum of 14.29 MB/s. There should be further investigations into storage speeds and bottle necks if this limit is even closely approached. Downsides to onboard storage include a possibility of added weight, no ability to react in real time to information observed, such as forest fire prevention or downed powerlines.

Live streaming was not investigated in this project. There are large benefits to having real time information of the mission, especially for long endurance missions such as the one for the Peregrine 1, but these benefits come with extra complexity.

2.1.7 Post Processing

Post processing was removed from the authors scope due to the complexity of a full scale mapping system, among other tasks. For optical imagery, there are open source processing algorithms available online, but it is beleived that these require a substantial amount of entry knowledge in addition to a powerful computer. There are many complete softwares that advertise photogrammetry post processing of images. Agisoft and Pix4D are two seen in literature often [10]. Others include Correlator 3D and ODM.

2.1.8 Mapping Function Considerations

All mapping theory sections above are essential considerations for a full design and implementation of a mapping system for an aerial mission. A flow chart was created to outline these considerations and place them relative to where they are most significant in a chronological overview of the full mapping process.

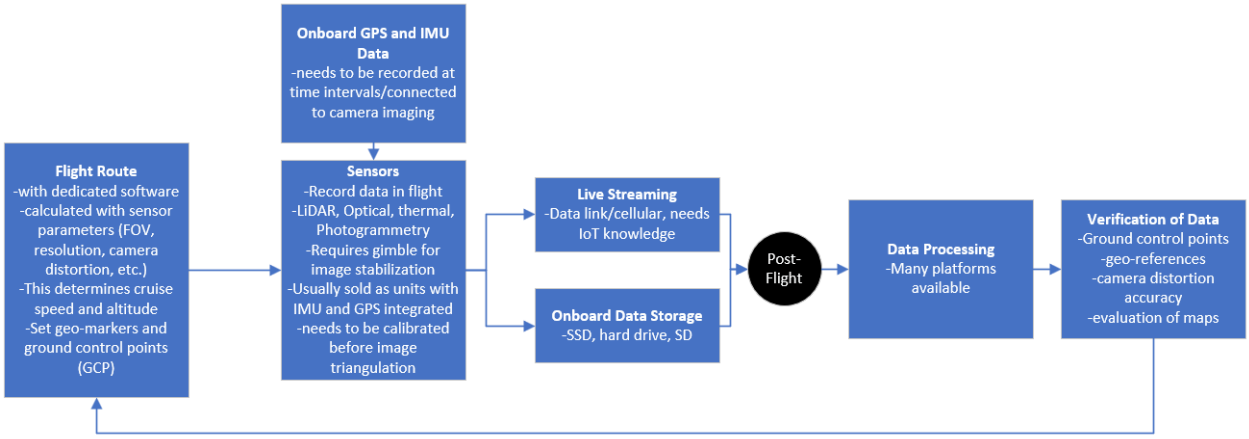

Figure 5: Mapping function considerations flowchart

2.2 Mission Profile

The selection of the mission profile was opened to the entire capstone group for ideas. It was identified early on that our platform cruise speed is much higher than the cruise speed seen in research papers of similar scope [11] [12] [13] [14]. To select the Peregrine 1 mission, the largest consideration was how the speed of the platform can be used to the advantage for the mission.

From similar off-the-shelf products, the 34.5 m/s cruising speed of the Peregrine 1 sits at the upper limit of most commercially available mapping drones. Some examples drones marketed as “high-speed” include the line from JOUAV [15], the WingtraOne Gen II [16], the GAOTek High Speed Drone [17], and the Delair UX11 [18]. Notably, all but a few platforms from JOUAV have slower cruising speeds than the Peregrine 1.

2.2.1 Considerations

The main advantage of a faster cruising speed than commercially available products is the ability to capture large amounts of data quickly. Pairing this with the long endurance solar powered goal of the

mission, there is a large potential for huge swaths of lands to be imaged and mapped in a short period of time. This shifted the focus from site planning and urban development to a broader focus on environmental and forest monitoring.

Some disadvantages are the requirement for higher quality cameras to reduce the effects of motion blur. A mechanical shutter is also recommended at these speeds, which is discussed in *2.3.1 Sensor Trade Study*.

2.2.2 Profile Selection

A concept was proposed to focus the mission on long distance powerline corridor monitoring. An investigation into the costs of powerline corridor clearing found that in 2018, 15.5 million dollars were spent managing tree growth along powerlines [19]. Additionally, as recent as 2011 it was found that a highly toxic herbicide called Agent Orange was used in powerline and railroad vegetation clearing in northern Canada between 1950 and 1970 [20]. Although it is unknown the exact method of powerline corridor vegetation clearing in Canada currently, it is proposed that low-cost and long-range UAV mapping could assist in identifying problem areas well before they appear, allowing a more targeted approach to powerline corridor clearance.

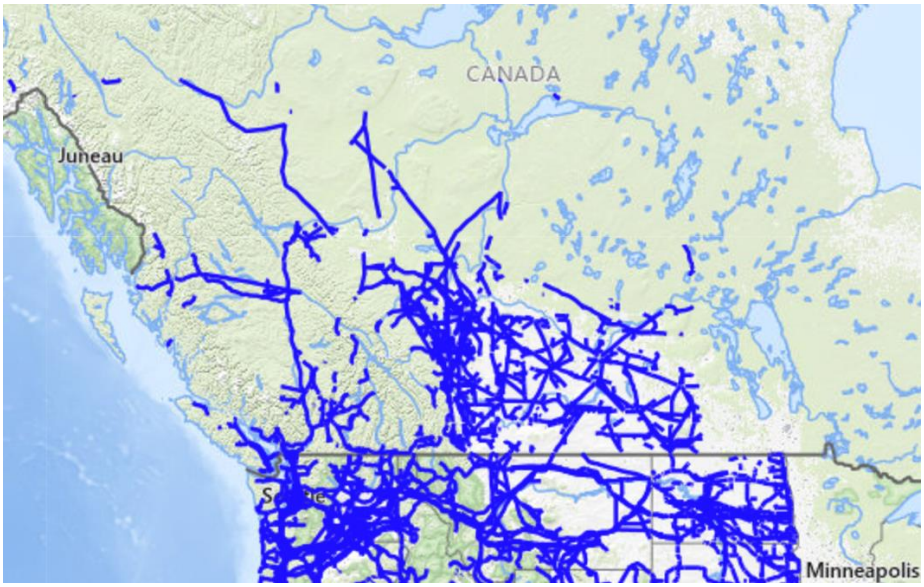

Figure 6: Powerline Corridors in the western United States and Canada [21]

The exact mission profile for the current year is described more in the technical report of the Advanced Design Engineer.

2.3 Mapping Hardware for Peregrine 1

From the literature review and a meeting with Lead Engineer Peter Liu, a narrower scope was defined for the Systems Engineer. For the Peregrine 1, the goal was set to, “deliver the complete hardware package to allow for optical aerial imagery. Ensure the hardware selected will allow for photogrammetry in the future.”

Since image processing and camera calibration for photogrammetric purposes is no longer in the scope, an off-the-shelf mapping camera was sought to reduce the integration complexity.

2.3.1 Sensor Trade Study

To determine the type of sensor that would be implemented in the mapping module to further guide the camera selection, a trade study was conducted using information from various sources and vendor specification sheets.

Table 1: Qualitative Trade Study Information

Sensor	Uses in Aerial Mapping	Strengths	Weaknesses	Perceived Complexity	Weight	Cost (min.)
LiDAR	-accurate elevation and 3D capture	-3D point cloud and accuracy	-price and complexity	High	780g-2kg incl. gimbal	$5000
RGB	-many general uses -urban planning -forest management	-open-source photogrammetry -DIY well documented		Medium	400g-1kg incl. gimbal	$300
Thermal	-environmental conditions -wildlife	-wide angle IR is niche and expensive	-software for processing limited -wide angle IR is more expensive	High	113g w/o gimbal [22]	$900
Multispectral	-agriculture -coastal boundaries	-wider range of applications	-software for processing may be limited	Medium	200 w/o gimbal [3]	$1000
Hyperspectral	-Mineral deposits -geology -ground cover -and multispectral	-even wider range of applications	-software for processing may be limited	Medium	790g incl. gimbal [23]	Too much

The qualitative results of the trade study were numbered and resulted in the selection of an RGB sensor as the basis of the mapping module. The main advantage of a three-band optical sensor was the relative cost compared to other options and the vast database of DIY projects to consult. It is important to note that this decision was eventually overturned by the other systems engineer, described in *2.3.3 Camera Selection*.

2.3.2 Optical Sensor Parameters for Mapping

Further research was done on the various intrinsic lens properties and camera specifications and their effect on the mapping mission. The qualitative effects were compiled from many sources in literature, online forums and discussions.

The numerical parameters described are preliminary estimates based on market cameras within each price range. The values do not necessarily represent a value that should be sought, but as a common parameter for a camera of that price point. These results are a starting point for further literature review into exact camera parameters used and their respective results for the mission.

Table 2: Camera Sensor and Lens Property Parameter Considerations

Parameter	Importance	Budget Requirement < $500	Mid-Range Requirement < $1500
Resolution	Improves ground sampling distance	16-24 MP	30-50 MP
Shutter Type	Mechanical shutter captures all light at once	Rolling	Mechanical
Shutter Speed	Affects Motion Blur	1/1000s to 1/2000s	1/2000s to 1/8000s (60KTAS)
Sensor Size	Directly affects GSD	22x15mm	Full-Frame 36x24
Image Stabilization	Motion Blur, image sharpness	Minimal	Gimbal Integration or in-body stabilization
Iso Range	Low light performance, shadows, overcast	ISO 100-6400	ISO 100-32000
Weight and Volume	For mission duration	Lower, <1kg	Higher, <1.5kg
Lens FOV	Quality and Edge Distortion	24-35mm	24-50mm prime lenses
GPU and IMU Integration	Required for geotagging (Hot shoe adapter)	Required	Required
Sensor Read and Storage Write Speed	Critical for current cruise speed	Depends on storage method	Depends on storage method

2.3.3 Camera Selection

Due to scope changes for the author, the other Systems Engineer was tasked with completing a trade study between specific cameras and their sensor parameters. All research and study information were given to the other Systems Engineer, but little input was given for the final selection.

3.0 LANDING GEAR DESIGN

For the landing gear, a consultation and review of previous work was done. Previous implementations were considered for transferable and reusable features. Unfortunately, in the 2021-22 and the 2020-21 year, a VTOL design was implemented. This design had no considerations for the specific loads seen in the landing of a conventional design in addition to the lack of wheels. In previous years to these, the landing

gear was a fixed, off-the-shelf product. From these findings, a clean sheet design was pursued to align with the additive manufacturing requirements of the current year. Design analysis from previous years was consulted and used where possible.

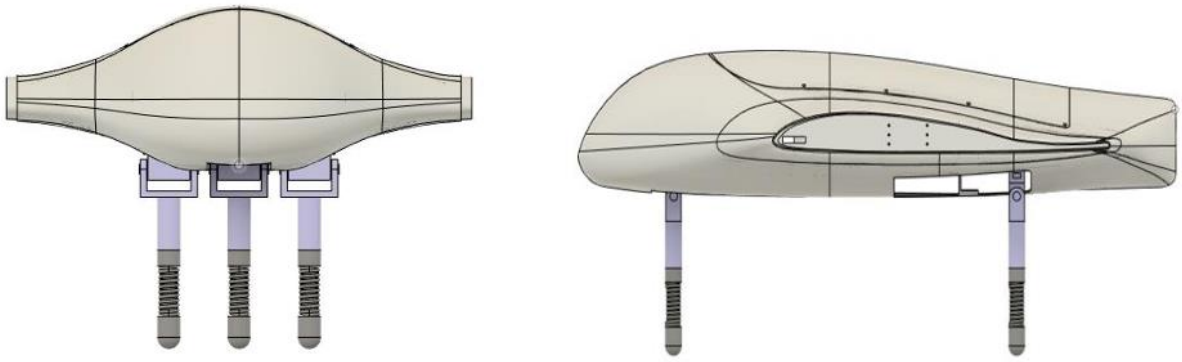

Figure 7: Proposed landing gear design for VTOL configuration [Winter technical report Qi Wei]

The semester goals included the physical testing of the retraction system, print, and loads testing of the struts and the basis of a shock system designed. Due to a high-risk issue with the Peregrine 1 Catiav5 model, this progress fell short of expectations.

3.1 Concepts

Three initial concepts were proposed. The first, a fixed landing gear design using the proven fuselage mounting and ground contact points. The second design was a retractable configuration which attempted the same fuselage mounting and ground contact points as before. Due to its retraction path into the fuselage and through structural members, and its volume requirements in the center of the fuselage, a third option was proposed to mitigate these issues. The third configuration is a retractable gear whose ground contact points were kept constant but fuselage mounting points altered.

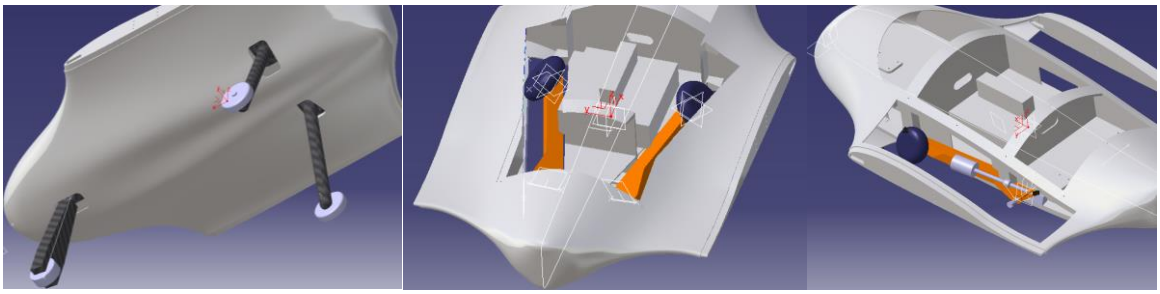

Figure 8: Implementations of the fixed (left), configuration 1 (middle), and configuration 2(right) landing gears

3.1.1 Previous Configurations and Considerations

The retract system designed in the 2021-22 year was desired to be used in the design, but there were a few errors identified in the hand-off letters. It was identified that the servo selected would not fit within the OML after retraction. Additionally, the servo torque was determined based on only the static retraction of the gear and did not consider aerodynamic loads during flight. The stall torque of the chosen servo was $19.3\ [kg * cm]$ and the calculated maximum torque needed for a stationary retraction of the

landing gear was determined to be $15.1\ [kg * cm]$ [24]. This represents a safety factor of only 1.27 before aerodynamic loads were applied.

In addition to the retraction system, a preliminary design of a spring shock was designed for the landing gear structure by the 2022 Systems Engineer. This design is used as the starting point for the current design, but further literature review and testing is needed. The only parameter calculated was the maximum stroke energy due to the VTOL configuration and transverse loads from conventional landing were not considered [25].

3.1.2 Initial Concept Design

For the conventional aircraft platform, the initial idea was to repurpose the wheels used in the pre-VTOL configuration years, keep the same fuselage mountain points as a starting place for stress analysis, and keep the same ground contact points as to not affect the stability during taxi and takeoff. The focus was to get a general sense of geometry based on these constraints and design the simplest structure between the ground and fuselage. The general flow of structural analysis this year is to pass all structural members to the Stress and Structure Engineers, who will mesh, analyze, and perform FEA. If the structure is sufficient based on expected loads from the Loads Engineer, it will be forwarded to the MSDO Engineer for optimization. After this iterative cycle, suggestions would be cycled back to the author for further design changes.

For the retractable landing gear configurations, a simple trunnion-pin design was implemented, where an axle could run through the trunnion of the landing gear and allow the required retraction path.

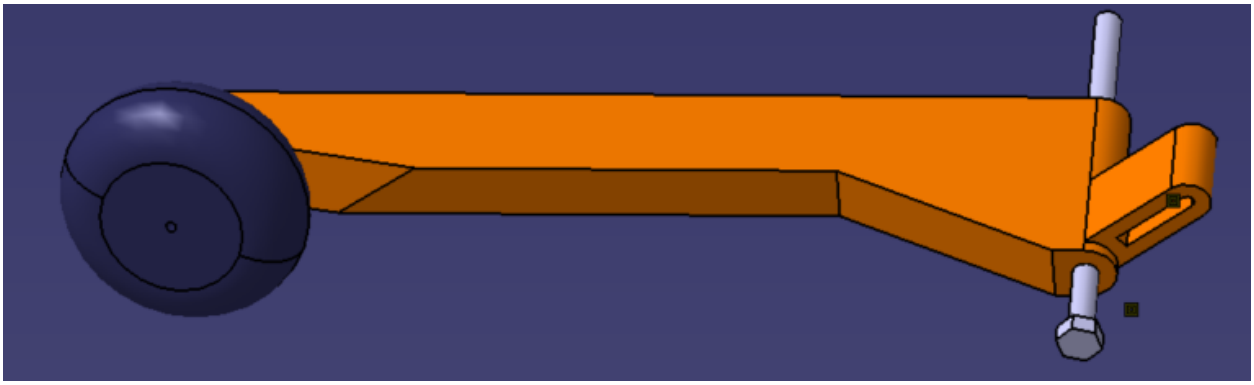

Figure 9: Retractable LG Trunnion and Pin demonstration

The geometric positioning of the landing gear within the structure was done by trial and error, ensuring that the position of the trunnion relative to the fuselage will allow the geometry of the landing gear structure to be properly oriented in all states. The wheel needs to be at the desired ground contact position and orientation at one end of the retraction path and a desired stowage position on the other end of the retraction path.

Due to the narrow volume of the root fairing, the wheel only can be enclosed within the OML on retraction in certain orientations. This was the main constraint for the trunnion orientation.

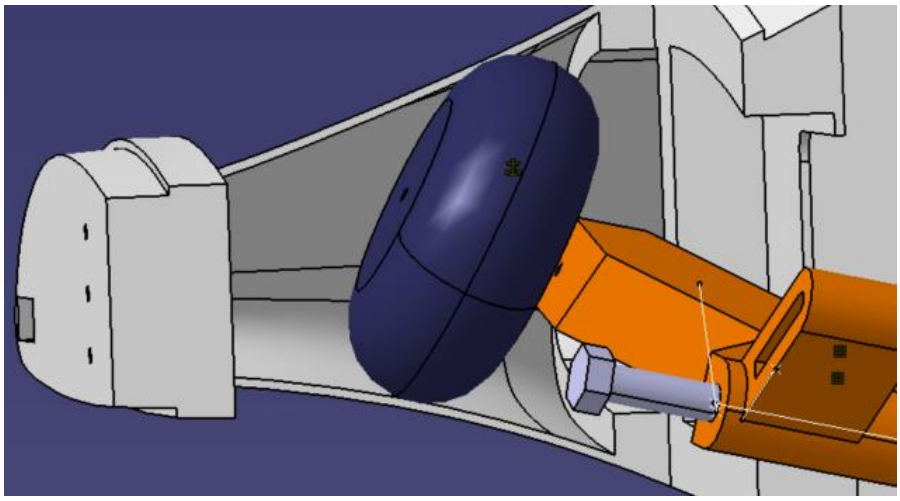

Figure 10: Wheel clearance between skin in fuselage root fairing

As mentioned previously, the exact structure parameters of the landing gear were of low concern during the initial placement phase as many iterations were expected upon results from Stress, Structure, MSDO, and Loads Engineers.

3.1.3 Masterlines Model Implementation

To begin with the structural considerations of the landing gear, the preliminary models were to be integrated into the Peregrine 1 model for subsequent analysis from other Engineers. There were some complications with the Catia model during this semester which resulted in the delay of this process. As of writing this report, no structural analysis has been performed on any of the configurations.

3.2 Shock

A shock absorbing system to be implemented into the structure of the landing gears is necessary for the longevity of the platform. Preliminary hard landing loads from the Loads Engineer estimate peak loads of 8G on the Peregrine 1 with no shocks.

Current ideas for this project include performing a proper spring-mass-damper analysis of the loads seen in the ideal landing configuration and the worst case of hard landing loads. Off the shelf oleo struts have been considered as an easy solution with a weight penalty of almost 500 grams for only the oleo struts and wheel axles [26]. This will be considered if significant problems arise with the design of a suitable custom damping system.

The previous design with one spring as the shock system is at risk of inducing bounced landings in the aircraft. To account for this, damping characteristics must be added. Current interests are the implementation of orifices on both sides of the plunger in the cylinder to restrict airflow in either the positive or negative compression state of the shock. Combined with a top and negative spring, similar to how high-end bicycle and motorcycle shocks are designed, this may allow a very lightweight and cost-effective solution.

Much of the progress on the shock system is from the first month, before the additional tasks of Catia modelling were known to the author.

3.3 Retraction System

The design of the retraction system is modelled after a design found by one of the previous Systems Engineers, Qi Wei. The design employs a lead screw actuator which moves a positioning tool along the axis of the actuator. With the rotation axis of the LG below the actuator, it can be pivoted with the positioning tool.

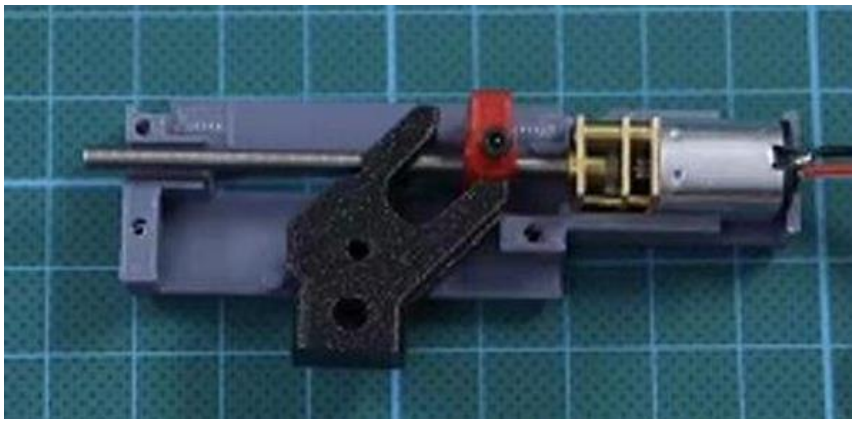

Figure 11: Retraction concept using lead screw actuator [27]

Currently, the retractable landing gear and its mechanism is paused for the project. Due to the change of scope described in *4.0 CATIA MODELLING*, continuing to develop this mechanism alongside other responsibilities presents a high risk that timelines will not be reached. Time permitting, this mechanism will be further developed for future use due to its advantages of high torque, precise positioning, and the inability to reverse drive the actuator upon hard landing or aerodynamic loads.

3.4 Performance Study

To properly evaluate the trade-offs between a fixed and retractable landing gear configuration, the author proposed a performance study between the fixed and retractable configuration 2 designs. Using parasitic drag properties retrieved from CFD analysis and the mass properties of each configuration, the performance would be compared between the increased drag, reduced weight fixed gear and the reduced drag, increased weight retractable gear.

The models were produced for both configurations but were unable to be integrated into the Peregrine 1 model. Additionally, CFD was unable to be performed on the P1 model due to geometry issues. Mass properties were estimated for both configurations, described below.

3.4.1 Mass Properties

The assumptions used for the preliminary estimation of landing gear mass properties were as follows:

- The landing gear door will weigh approximately the same as the skin it will replace.
- The displaced structure of the landing gear retraction path will be reallocated to the trunnion support system.
- Weight of the wires for the actuators is negligible.
- The structure of the retractable LG will weigh approximately 10% more with the trunnion and retraction lug.

- The shock absorber will be the same for either concept.

These assumptions allowed a weight estimation for both gears. The mass of the fixed gear was calculated using the volume properties from Catia and the density of PETG. The hardware was selected from standard hardware found on McMaster-Carr, and their weights estimated with a hardware weight calculator provided by Portland Bolt [28] [29]. The results are shown in Table 3 below.

Table 3: Preliminary weight estimations for fixed vs. retractable gears

Component	Retractable Weight	Fixed Weight
Wheels	32g	32g
Axles (1x#2x1.5" and 2x#5x1.5" bolts)	~10g	~10g
NLG Solid ($10.18in^3$)	$215g * 10\% = 236g$	215g
MLG Solid (2x$5.877in^3$)	$244g * 10\% = 268g$	244g
Motor and Lead Screw	~60g	N/A
Trunnion Bolt	~35g	N/A
Total Weight	**~640g**	**~500g**

It is important to note that the volume-density weight estimations for the NLG and MLG structure assume 100% infill as a 3D print parameter. It is likely that after the infill settings are determined by Additive Manufacturing Engineers and the MSDO Engineer optimizes the structure, the structure will weigh less. The relative weight between each structure should remain relatively similar. An approximately 28% increase in weight should be expected to transition to a fixed landing gear design.

4.0 CATIA MODELLING

Throughout the semester, a problem with the previous CatiaV5 model of the Peregrine 1 was identified. One of the Additive Manufacturing Engineers was employed to assist in getting the model to a usable state. The model was identified to have several fatal flaws in its design, at which point the author was requested to assist with the rectification of these problems.

The work performed on the Catia model is further described in a technical document and technical memo.

4.1 Problem Identification

Working with the Additive Manufacturing Engineer who was appointed to help with the model, several critical issues were identified on the model. Specific issues are addressed in the technical documentation for the CatiaV5 reconstruction.

It was decided that a complete reconstruction of the Peregrine 1 model was essential for the project.

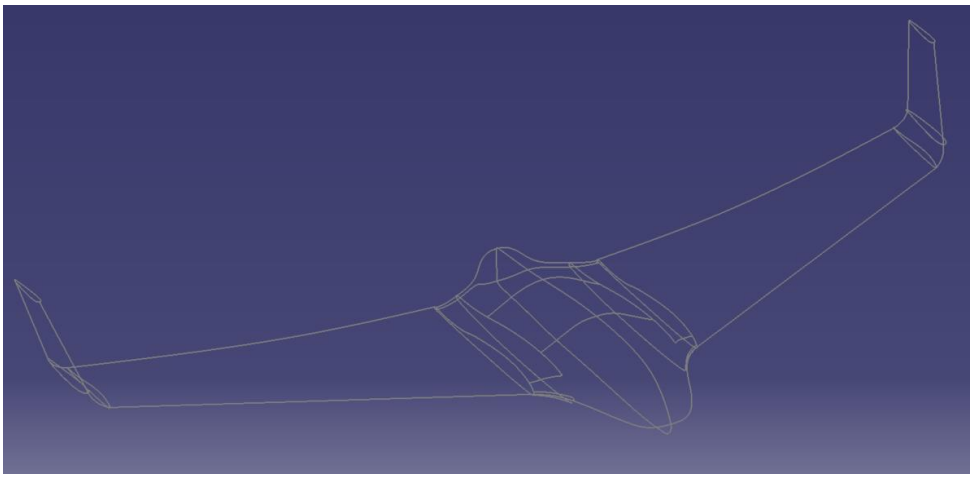

Figure 12: Wireframe of P1-OML Surfaces

4.2 Reconstruction

To ensure the P1 OML was true to the previous initial design, a CATPart body containing the original outer surfaces of the Peregrine 1 was used as the reference material for all future construction.

4.2.1 Surface Reconstruction

In the P1 surface geometry file, there were surface geometries that halted the 3D construction. The connection between some adjacent surfaces was broken, there were several holes in surfaces, and there were overlapping surfaces.

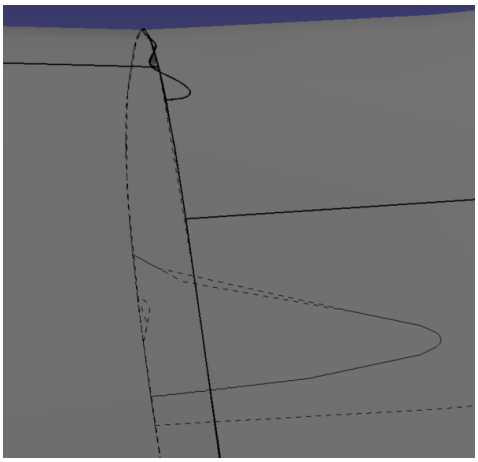

Figure 13: Voids and Overlapping Surfaces on the P1 Surface Geometry

The objective for the surface mending is to get the surfaces to a state where the *Join* or *Heal* commands can be used in the *Generative Shape Design* workbench in Catia.

For overlapping surfaces, the overlapping section was trimmed from one of the two overlapping surfaces. This was accomplished by creating a closed sketch on the desired splitting plane. Using the *Fill* command on this sketch, a splitting surface was created. The *Split* function was used to cut the work surface with the splitting surface and the desired side of the splitting plane was specified to be kept. In Figure 14: Overlapping Surface Trimming by Splitting Surface below, the splitting surface is shown in blue, and the

work surface is outlined in orange. This overlapping surface feature is visible in Figure 13: Voids and Overlapping Surfaces on the P1 Surface Geometry above.

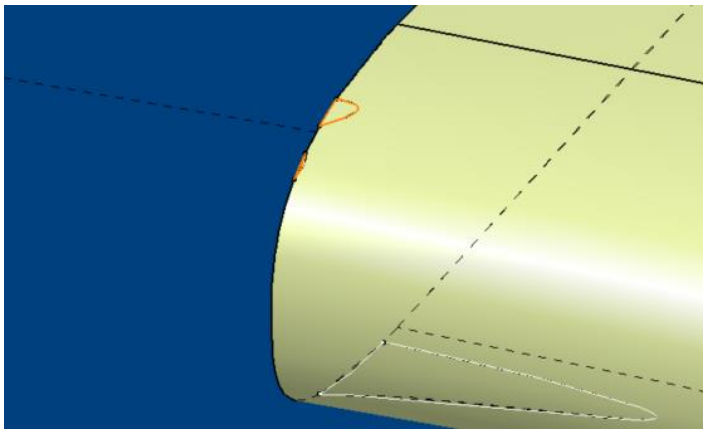

Figure 14: Overlapping Surface Trimming by Splitting Surface

Voids in the surface were mended by projecting the edges of the bordering surfaces to the workspace using the *Spline* tool. Once a closed sketch was obtained, it was made into a surface using the *Fill* tool.

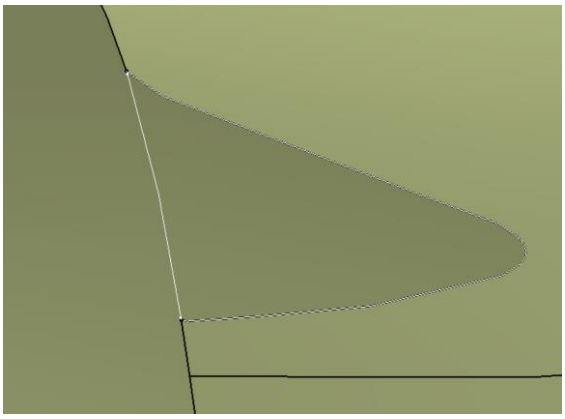

Figure 15: Void Repair for Surfaces

Once the surfaces were fine-tuned and modified, the *Join* command was used to join and heal intersections between the many individual surfaces, including those that were created to fill voids. This single resultant surface was used as the reference OML for all proceeding 3D part construction requiring the OML as a reference.

4.2.2 Wingskin Reconstruction

Using the geometrical set containing the reference OML, a solid Wing was created using the *Close Surface* command in the *Part Design* workbench.

To hollow the solid body to be used as the wingskin, Boolean operations in Catia were used. The objective is to create a smaller wingskin body within the full sized one and subtract the intersecting volume of the small body from the large. Several planes were constructed down the length of the wing and the *Offset* tool in the *Sketch* workbench was used to designate an offset value of the OML projection on each plane. This offset value was set as a variable parameter to allow for easy wingskin thickness changes in the future.

The closed profile of these planes can be chained together into a single surface using the *Multi-Sections Surface* tool in the *Generative Shape Design* workbench.

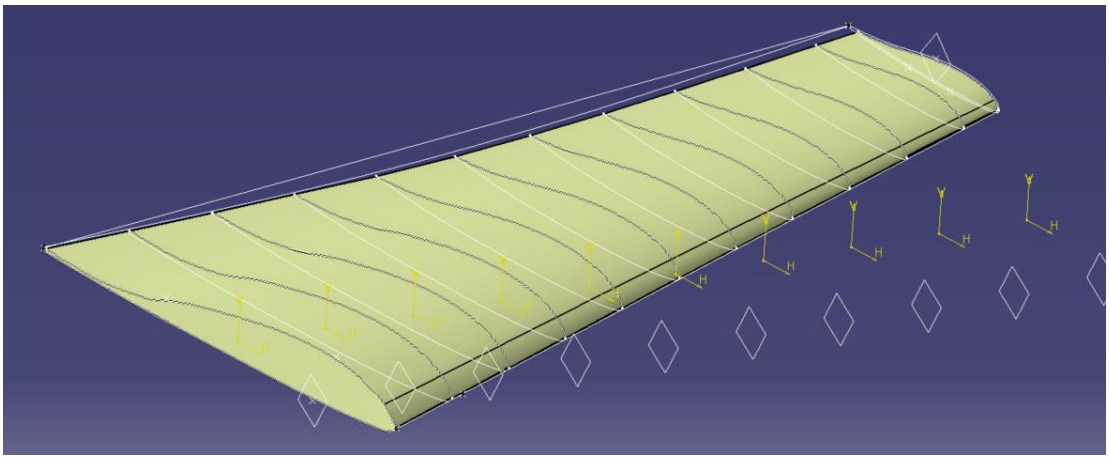

Figure 16: Multi-Sections Surface of the OML Profile Projection Offset Sketches

This offset surface was turned into a solid body using the *Close Surface* tool similarly to the full-sized surface. The Boolean operator Subtract was used to remove the interior solid from the exterior.

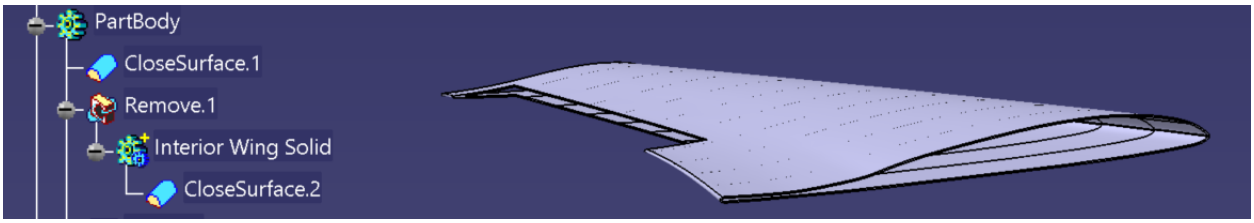

Figure 17: Hollow Wingskin Model

4.2.3 Additional Parts, Assembly, and Offboarding

The elevon and winglets were constructed similarly to the wing. Using the fuselage part reconstructed by Tim Speyer, a full OML component assembly file was created in Catia. Components were constrained to their appropriate position and the resultant OML was compared with the previous model to verify the reconstruction accuracy.

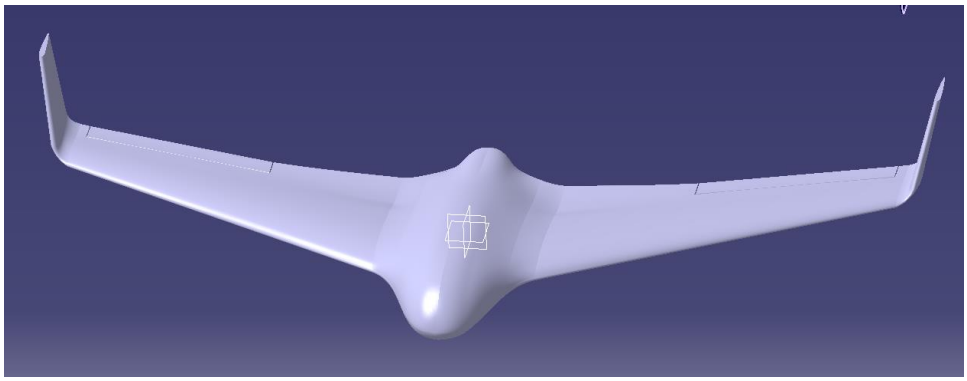

Figure 18: P1 OML Assembly Model

Once the OML was reconstructed, technical documentation was created by the author describing in detail the challenges faced, and the solutions employed for future students working on the BWB UAV Capstone. The model was transferred back to Masterlines and work on the Catia model ceased.

5.0 CONCLUSION

The progress of the core responsibilities was unsatisfactory compared to the initial semester goals. The additional work on the Catia modelling took a significant amount of time to resolve. Future goals have been reconsidered based on how essential they are to the success of the Peregrine 1 and the available time in the semester.

5.1 Mapping Module

The mapping module objective was redefined to require that the Peregrine 1 be fitted with the required hardware for aerial imagery and that this hardware be capable of photogrammetry in the future. This rescope will allow the System Engineers to focus on high level system requirements without having to consider the technical side of camera sensor calibration for use in photogrammetry software and data verification.

The camera has been selected by the other Systems Engineer. Mounting hardware will need to be designed or selected for the camera housing. Modifications will need to be recommended to the Masterlines Engineer to allow the camera to have a porthole on the underside of the aircraft. Additionally, anti-vibration solutions will be considered. Lastly, the integration of the camera into the avionics system will be determined by working with the Avionics Engineer. There needs to be communication established between the onboard computer and the camera, likely through a hot-shoe adapter.

5.2 Landing Gear

From the delay in landing gear progress from the work done on the Catia model, it was decided that the retractable system would be postponed unless progress is rapid. The goal for the semester is to have the fixed landing gear model verified by Stress and Structure Engineers and printed for physical testing early in the winter semester.

The shock for the landing gear needs significant analysis before implementation. The design should be chosen and numerically verified for damping characteristics prior to being implemented on the landing gear. In addition to this, physical testing is planned to be completed on the landing gear and shock under the expected loads.

For integration into the fuselage structure, the Masterlines Engineer and Avionics Engineer will be consulted for the structural and electrical interfaces, respectively.

The retraction system is planned to be further developed for future years, time permitting. Alongside this design work the proposed fixed versus retractable landing gear performance study is planned to be completed for future years.

5.3 Additional Tasks

The elevon integration will be verified and enacted prior to wind tunnel testing. This work will be done alongside the Avionics Engineer.

5.4 Recommendations

To ensure that the integration of all systems can be completed effectively, the Masterlines Engineer should continue receiving assistance from other members of the team. Additionally, to ensure that the project objective is met, the structure of the Peregrine 1 needs to be finalized and modelled as soon as possible.

6.0 REFERENCES

[1] A. Bowers, "Blended Wing Body: Design Challenges for the 21st century," NASA, 200.

[2] YellowScan, "LiDAR Point Cloud Basics," 2024. [Online]. Available: https://www.yellowscan.com/knowledge/lidar-point-cloud-basics/. [Accessed 03 12 2024].

[3] Spectral Devices, "Multispectral Drone Cameras," Spectral DEVICES Inc., 2024. [Online]. Available: https://spectraldevices.com/collections/multispectral-drone-cameras. [Accessed 03 12 2024].

[4] S. Castillo-Girones and R. Van Belleghem, "Detection of subserface bruises in plums using spectral imaging and deep learning with wavelength selection," *Postharvest biology and technology,* vol. 207, 2024.

[5] NOAA Ocean Exploration, "Photogrammetry," National Oceanic and Atmosperic Administration, 2024. [Online]. Available: https://oceanexplorer.noaa.gov/technology/photogrammetry/photogrammetry.html#:~:text=Photogrammetry%20is%20a%20method%20of,other%20products%20like%20photomosaic%20maps.. [Accessed 03 12 2024].

[6] F. B. K. Francesco Nex, "UAV for 3D Mapping Applications: A Review," *Applied Geomatics,* p. 28, 2014.

[7] National Part Service, "Photogrammetry," NPS.gov, 29 10 2018. [Online]. Available: https://www.nps.gov/subjects/geohazards/photogrammetry.htm. [Accessed 03 12 2024].

[8] Wingtra, "Ground sample distance explained and why it matters," Wingtra, 2024. [Online]. Available: https://wingtra.com/surveying-gis/ground-sample-distance/#:~:text=Technically%2C%20GSD%20is%20the%20distance,cm%20square%20on%20the%20ground.. [Accessed 03 12 2024].

[9] C. M. C. E. Rupnik, "Simulation and Analysis of Photogrammetric UAV Image Blocks - Influence of Camera Calibration Error," *Remote Sensing,* vol. 12, no. 1, p. 22, 2020.

[10] H. W. A. R. K. E. D. W. B. S. Muhammad Mukhlisin, "Rapid and low cost ground displacement mapping using UAV photogrammetry," *Physics and Chemistry of the Earth,* vol. 130, 2023.

[11] J. Zhang, "UAV-Borne Mapping Algorithms for Low-Altitude and High-Speed Drone Applications," *Sensors,* vol. 24, no. 7, 2024.

[12] J. S. A. K. M. L. Miloš Rusnák, "Template for high-resolution river landscape mapping using UAV technology," *Measurement,* vol. 115, pp. 139-151, 2018.

[13] C. G. M. A. Alvarez Larrain, "Participatory mapping and UAV photogrammetry as complementary techniques for landscape archaeology studies: an example from north-western Argentina," *Archaeological Prospection,* vol. 28, no. 1, pp. 47-61, 2021.

[14] R. A. Fernandes, Assessment of UAV-based photogrammetry for snow-depth mapping: data collection and processing, Canada: Natural Resources Canada, Geomatics Canada, 2017.

[15] JOUAV, JOUAV Unmanned Aircraft System, 2024. [Online]. Available: https://www.jouav.com/products/cw-80e.html. [Accessed 03 12 2024].

[16] Wingtra, "WingtraOne Gen II," 2024. [Online]. Available: https://wingtra.com/mapping-drone-wingtraone/?srsltid=AfmBOorhxFIkqJO6_xVnv1ClPajNBNPzUQPcAYMmXJGdZwdAX2jlDX2C. [Accessed 03 12 2024].

[17] GAOTek, "GAOTek Autonomous High Speed Surveillance VTOL Drone Fixed Wing UAV For Mapping," 2024. [Online]. Available: https://gaotek.com/product/gaotek-autonomous-high-speed-surveillance-vtol-drone-fixed-wing-uav-for-mapping/. [Accessed 03 12 2024].

[18] DELAIR, "Delair UX11 the smartest Mapping Drone," 2024. [Online]. Available: https://delair.aero/delair-commercial-drones-2/professional-mapping-drone-delair-ux11-2/. [Accessed 03 12 2024].

[19] R. Jones, "Years of reduced spending on tree clearing preceded major N.B. Power outage," CBC News, New Brunswick, 2023.

[20] T. Noakes, "Canada and Agent Orange," The Canadian Encyclopedia, 23 07 2021. [Online]. Available: https://www.thecanadianencyclopedia.ca/en/article/canada-and-agent-orange. [Accessed 03 12 2024].

[21] S. P. Finn, "Powerline Corridors in the Western United States and Canada," Forest and Rangeland Ecosystem Science Center (FRESC) Headquarters, Corvallis, OR, 2023.

[22] Teledyne FLIR, "FLIR Vue Pro R," FLIR, 2024. [Online]. Available: https://www.flir.ca/products/vue-pro-r/?vertical=suas&segment=oem. [Accessed 03 12 2024].

[23] HAIP, "Hyperspectral camera drone black bird v2," HAIP Solutions, 2024. [Online]. Available: https://www.haip-solutions.com/hyperspectral-cameras/hyperspectral-camera-drone/. [Accessed 03 12 2024].

[24] Q. Wei, "Systems Engineer - 2 Winter 2022 Technical Report," Dept. of mechanical and aerospace engineering, Carleton, Ottawa, 2022.

[25] Q. Wei, "SYSTEMS ENGINEER - 2 FALL 2021 TECHNICAL REPORT," Dept. of Mechanical and Aerospace Engineering, Ottawa, 2021.

[26] Turbines RC, "JP Hobby ER-150 15mm Scale Metal Oleo Struts (single nose strut) (Boomerang Elan V2 2.13m or planes up 20kg)," 2024. [Online]. Available: https://www.turbines-rc.com/en/struts/3176-jp-hobby-er-150-15mm-scale-metal-oleo-struts-single-nose-strut-boomerang-elan-v2-213m-or-planes-up-20kg.html. [Accessed 04 12 2024].

[27] KendinYap, Director, *Making Retractable Landing Gear for RC Model Airplanes. DIY Electric Retract.* [Film]. Youtube, 2021.

[28] McMaster-Carr, "McMaster-Carr Catalog," 2024. [Online]. Available: www.mcmaster.com. [Accessed 20 10 2024].

[29] Portland Bolt & Manufacturing Company, LLC, "Bolt Weight Calculator," 2024. [Online]. Available: https://www.portlandbolt.com/technical/tools/bolt-weight-calculator/. [Accessed 22 10 2024].